Supramolecular Chemistry

International Edition: DOI: 10.1002/anie.201605454
German Edition: DOI: 10.1002/ange.201605454

Symbiotic Control in Mechanical Bond Formation

*Yuping Wang, Junling Sun, Zhichang Liu, Majed S. Nassar, Youssry Y. Botros, and J. Fraser Stoddart**

Abstract: *Since the advent of mechanically interlocked molecules (MIMs), many approaches to templating their formation using various different noncovalent bonding interactions have been introduced and explored. In particular, employing radical-pairing interactions between $BIPY^{\bullet+}$ units, the radical cationic state of 4,4′-bipyridinium ($BIPY^{2+}$) units, in syntheses is not only a convenient but also an attractive source of templation because of the unique properties residing in the resulting catenanes and rotaxanes. Herein, we report a copper-mediated procedure that enables the generation, in the MIM-precursors, of $BIPY^{\bullet+}$ radical cations, while the metal itself, which is oxidized to Cu^{I}, catalyzes the azide–alkyne cycloaddition reactions that result in the efficient syntheses of two catenanes and one rotaxane, assisted by radical-pairing interactions between the $BIPY^{\bullet+}$ radical cations. This procedure not only provides a fillip for making and investigating the properties of Coulombically challenged catenanes and rotaxanes, but it also opens up the possibility of synthesizing artificial molecular machines which operate away from equilibrium.*

For several decades, mechanically interlocked molecules[1] (MIMs), such as bistable catenanes and rotaxanes, have attracted[2] much attention from the broader community of scientists and engineers. Applications in directing the construction of molecular switches[3] and machines,[4] as well as in drug delivery[5] and molecular electronic devices,[6] are already well established. With our rapidly growing insight into molecular recognition and its use in aiding self-assembly processes, MIMs can now be synthesized in high yields by employing template-directed approaches[7] that rely on noncovalent bonding interactions. Among the redox-based approaches to templation, radical-pairing interactions[8] have been shown to provide a unique form of covalent assistance in the formation of mechanical bonds. Subsequent eradication of the radical-pairing interactions is more often than not followed by the formation of repulsive electrostatic interactions. In particular, recognition[9] between $BIPY^{\bullet+}$ units (the radical state of 4,4′-bipyridinium $BIPY^{2+}$) has captured our attention because of our interest in the syntheses of MIMs where the component parts repel each other in the final analysis.

Despite having alternative ways[10] to incorporate $BIPY^{2+}$ units into MIMs, the advantages of radical templation[8] are such that it allows the construction of catenanes and rotaxanes in the absence of electron-rich complementary units (Scheme 1), so that the resulting MIMs can have much simpler constitutions.[8b] More importantly, while the co-conformations of the catenanes and rotaxanes, under reducing conditions, are controlled by stabilizing radical-pairing interactions, Coulombic repulsions play an important role in

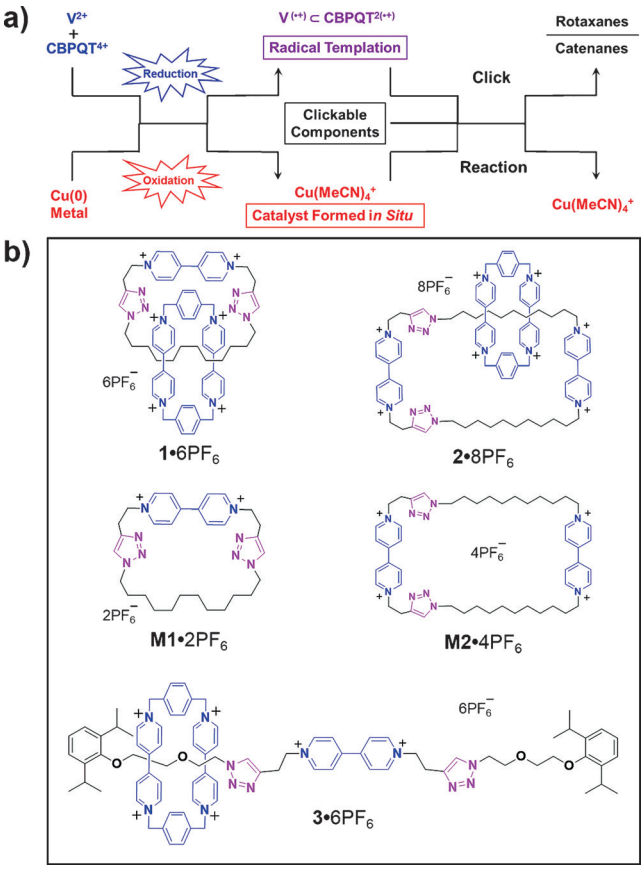

Scheme 1. a) Design strategy relating to a cascade approach for preparing radical-templated MIMs such as rotaxanes and catenanes by CuAAC, where Cu metal exhibits a domino-type mechanism during the reaction. b) Structural formulas of compounds **1**·6 PF_6, **2**·8 PF_6, and **3**·6 PF_6 synthesized using the radical procedure described in this paper. Macrocycles **M1**·2 PF_6 and **M2**·4 PF_6 are reference compounds.

[*] Y. Wang, Dr. J. Sun, Dr. Z. Liu, Prof. J. F. Stoddart
Department of Chemistry, Northwestern University
2145 Sheridan Road, Evanston, IL 60208 (USA)
E-mail: Stoddart@northwestern.edu
Dr. M. S. Nassar
Joint Center of Excellence in Integrated Nano-Systems (JCIN)
King Abdulaziz City for Science and Technology (KACST)
P.O. Box 6086, Riyadh 11442 (KSA)
Y. Y. Botros
PanaceaNano, Inc.
2265 East Foothill Boulevard, Pasadena, CA 91107 (USA)
Supporting information and the ORCID identification number(s) for the author(s) of this article can be found under http://dx.doi.org/10.1002/anie.201605454.

dictating the high-energy states adopted by the fully oxidized MIMs. This structure-dependent redox behavior allows us to access and explore the properties of systems far from equilibrium.[4b,c,11] It is of paramount importance, therefore, to develop new procedures that are user-friendly for constructing MIMs involving these radical species.

Copper(I)-catalyzed azide–alkyne cycloadditions[12] (CuAAC) are considered[13] to be amongst the most efficient forms of derivatization because of their short reaction times and high yields. More importantly, both the azide and alkyne components are amongst the most stable functional groups that can be introduced into a compound easily. Previously, we have demonstrated[8a] that the click reaction involving radical species (for example, forming mechanical bonds in viologen-based [2]rotaxanes) can be achieved by applying copper-free azide–alkyne cycloadditions.[14] This particular copper-free procedure, however, has several drawbacks, including slow reactions that can take up to several weeks to go to completion, resulting in low yields (commonly 30%), especially when reaction time periods are limited. Moreover, because the alkynes are internal ones in this particular approach, it follows that the constitutional options available to the alkyne components are limited, meaning that it becomes difficult to functionalize the resulting rotaxanes and it is nigh impossible to synthesize catenanes. Consequently, new methodologies for the efficient production of MIMs, employing radical templation,[8] are sorely needed.

In an attempt to address this bottleneck, we report a one-pot strategy for constructing radical-templated MIMs (Scheme 1a), wherein copper metal (diam $<425\,\mu m$) is utilized initially as the reducing agent to generate azide/alkyne-functionalized $BIPY^{\bullet+}$ radical cations ($\mathbf{V}^{\bullet+}$) from $BIPY^{2+}$ dications ($\mathbf{V}^{2+}$), while simultaneously, copper(0) is oxidized to copper(I), which is capable of catalyzing mechanical bond formation employing the CuAAC reaction in good yields and in a much shorter period of time. By employing this synergistic procedure, a series of new viologen-based rotaxanes and catenanes have been prepared (Scheme 1b), opening up the possibility of creating MIMs with considerably more complex structural features and capable of performing intricate functions.

At the outset we faced two major challenges in the shape of uncertainties when contemplating the operation of the domino-type mechanism postulated in Scheme 1a. First, to the best of our knowledge, no examples using Cu^0 metal to reduce viologens have been reported in the literature. Second, it has not been established whether the CuAAC reaction would be compatible with the presence of $BIPY^{\bullet+}$ radical cations. It was in the context of this uncertain background that we decided to begin our investigations (Scheme 2) by attempting to synthesize the [2]catenane $\mathbf{1}\cdot 6PF_6$ using a threading-followed-by-clipping strategy. We anticipated that, while the threading would be driven by the reductive formation of a trisradical tricationic inclusion complex in tandem with the oxidation of the Cu^0 metal to Cu^I, two successive [3+2] cycloadditions between a diazide and a bisalkyne, which would be catalyzed by the Cu^I ions, would lead to clipping, that is, cyclization to form a [2]catenane.

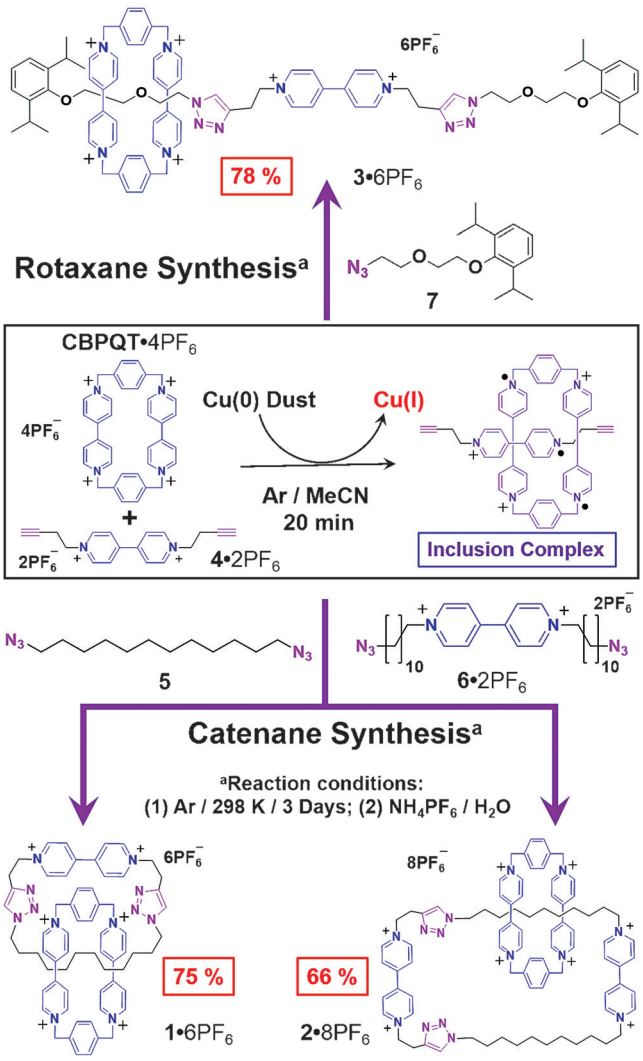

Scheme 2. Illustration of the cascade approach for creating radical-templated catenanes ($\mathbf{1}\cdot 6PF_6$ and $\mathbf{2}\cdot 8PF_6$) and the rotaxane $\mathbf{3}\cdot 6PF_6$. By treating the precursors $\mathbf{4}\cdot 2PF_6$ and CBPQT·$4PF_6$ with Cu^0 metal dust in MeCN, the $BIPY^{2+}$ units are reduced to their radical cationic states, resulting in the in situ formation of both Cu^I species and the trisradical inclusion complex $\mathbf{4}^{\bullet+}\subset CBPQT^{2(\bullet+)}$. A range of azide-functionalized compounds are used in the construction of the [2]catenanes $\mathbf{1}\cdot 6PF_6$ and $\mathbf{2}\cdot 8PF_6$ and the [2]rotaxane $\mathbf{3}\cdot 6PF_6$ employing CuAAC reactions.

Following the dissolution of the two viologen-based precursors, namely, $\mathbf{4}\cdot 2PF_6$ and CBPQT·$4PF_6$, in MeCN in a 1:1 molar ratio under an Ar atmosphere, an excess of Cu^0 dust (diam $<425\,\mu m$) was added to the solution. Upon stirring the reaction mixture for 20 min, the initial colorless solution gradually assumed a dark purple color, establishing (Figure S20) that Cu^0 dust can indeed reduce the $BIPY^{2+}$ units to their corresponding radical cations, leading to the formation of $\mathbf{4}^{\bullet+}\subset CBPQT^{2(\bullet+)}$. It is important to note, however, that this reduction is highly solvent (MeCN)-dependent, because other solvents, such as Me_2CO, produce no observable color change. We ascribe this marked solvent dependency to the fact that MeCN can stabilize the Cu^I ions by forming the tetrakis(acetonitrile) copper(I) complex, $[Cu(MeCN)_4]^+$. Next, without the need to filter off the excess of Cu dust,

1 equiv of 1,12-diazidododecane (**5**) is added to the reaction mixture in the expectation that it will react with the terminal alkyne groups in $\mathbf{4}^{\bullet+}$ forming the [2]catenane $\mathbf{1}^{6+}$. After stirring for 3 days at room temperature, air is introduced into the reaction mixture, resulting in the oxidation of the $BIPY^{\bullet+}$ units to their $BIPY^{2+}$ redox states. Following purification by column chromatography and counterion exchange, the [2]catenane $\mathbf{1}\cdot 6PF_6$, which can be obtained in yields as high as 75%, was subsequently characterized (Figures S1–S4) by HPLC, high resolution mass spectrometry (HRMS), and ^1H and ^{13}C as well as ^1H-^1H COSY NMR spectroscopies. It is important to note at this juncture that, compared to traditional CuAAC reactions[15] where either a catalytic amount of a relatively expensive Cu^I catalyst,[12b] or a complex system involving a Cu^{II} species and reducing agents is employed,[12a] the Cu^I species in this procedure is stoichiometrically generated in situ during the reduction step, and the reaction rates and yields are comparable with those (several hours and ≈85% yields) of the traditional methods.[12] This feature not only makes this copper-mediated technique neat and efficient, but also differentiates it from other copper-triggered CuAAC reactions that have been previously reported,[16] where a source of Cu^{II} species is also needed to generate active Cu^I catalyst by comproportionation ($Cu^0 + Cu^{II} \rightarrow Cu^I$).

Employing a similar synthetic strategy, a [2]catenane $\mathbf{2}\cdot 8PF_6$, incorporating an additional $BIPY^{2+}$ unit in the newly formed macrocycle interlocked with a $CBPQT^{4+}$ ring, has been prepared (Scheme 2) in a good yield (66%) from the trisradical tricationic complex $\mathbf{4}^{\bullet+}\subset CBPQT^{2(\bullet+)}$ and the diazide $\mathbf{6}\cdot 2PF_6$. The free macrocycles in [2]catenanes $\mathbf{1}\cdot 6PF_6$ and $\mathbf{2}\cdot 8PF_6$, namely $\mathbf{M1}\cdot 2PF_6$ and $\mathbf{M2}\cdot 4PF_6$, were also prepared to provide us with control compounds in subsequent experiments. Next, because research on MIMs these past two decades has revealed that [2]rotaxanes[17] have found much broader appeal than have [2]catenanes,[1c,18] when it comes to potential applications we considered it important that we also demonstrate the efficient synthesis of rotaxanes using the new copper-promoted radical cascade strategy. The [2]rotaxane $\mathbf{3}\cdot 4PF_6$, first proposed by us in an article[9a] has now been prepared (Scheme 2) in high yield (78%) from $\mathbf{4}^{\bullet+}\subset CBPQT^{2(\bullet+)}$ and the monoazide **7** using the copper-mediated cascade strategy.

The radical-based molecular recognition properties of the two catenanes and the rotaxane were first investigated by UV/Vis/NIR spectroscopy. Following the reduction of $\mathbf{1}^{6+}$, $\mathbf{2}^{8+}$, and $\mathbf{M2}^{4+}$ to their radical cationic states ($\mathbf{1}^{3(\bullet+)}$, $\mathbf{2}^{4(\bullet+)}$, and $\mathbf{M2}^{2(\bullet+)}$) by Zn dust in MeCN, all at the same concentration (20 μM), their absorption spectra were recorded at room temperature. The spectra reveal (Figure 1) that all three of the compounds have absorption bands around 550 nm, an observation which is characteristic of strong $BIPY^{\bullet+}$ radical pimerization.[9b,19] Particularly, in the case of the macrocycle $\mathbf{M2}^{2(\bullet+)}$, the two $BIPY^{\bullet}$ units have a strong tendency to form an intramolecular dimer $(BIPY^{\bullet+})_2$, giving rise to an absorption band centered on 855 nm. By contrast, however, when an additional $BIPY^{\bullet+}$ unit is introduced as in the case of $\mathbf{1}^{3(\bullet+)}$, a red-shifted absorption band at 1088 nm appears, indicating the formation of an intramolecular trisradical tricationic that is consistent with the co-conformation observed in the solid-state (super)-

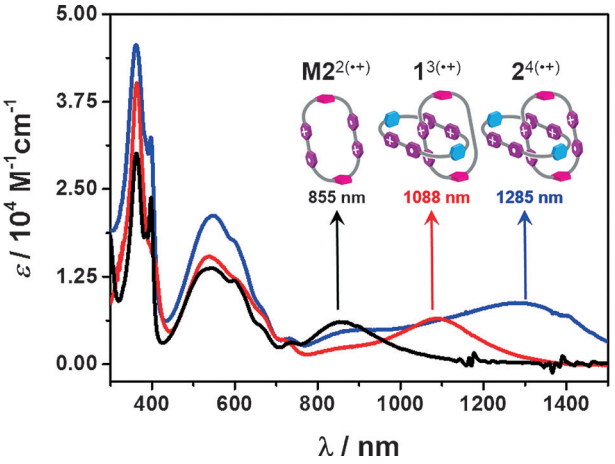

Figure 1. UV/Vis/NIR Absorption spectra of $\mathbf{1}^{3(\bullet+)}$, $\mathbf{2}^{4(\bullet+)}$ and $\mathbf{M2}^{2(\bullet+)}$ recorded in MeCN at 298 K at the same (20 μM) concentration. The wavelengths denoted by the arrows illustrate red shifts with increasing numbers of viologen units, commensurate with a narrower energy gap when a larger number of $BIPY^{\bullet+}$ radical cations interact with each other in solution.

structure of $\mathbf{1}^{3(\bullet+)}$ (see below). More significantly, perhaps, the UV/Vis/NIR spectrum of $\mathbf{2}^{4(\bullet+)}$ displays a further red-shifted absorption band at 1285 nm, an observation which clearly indicates the formation of an intramolecular tetracationic tetrakisradical rather than two pairs of radical dimers, as a result of the propensity for multi-state radical-pairing interactions in the nanoconfined structure of $\mathbf{2}^{4(\bullet+)}$. In summary, as the number of $BIPY^{\bullet+}$ units increases, from $\mathbf{M2}^{2(\bullet+)}$ to $\mathbf{1}^{3(\bullet+)}$ and ultimately to $\mathbf{2}^{4(\bullet+)}$, the corresponding radical-induced π-stack becomes more extended with consequent narrowing of the electron-migrating energy gap in concert with the absorption bands showing an approximately 200 nm red shift upon the participation of each of the four $BIPY^{\bullet+}$ units.

In an attempt to elucidate how the number of $BIPY^{\bullet+}$ units affects the recognition properties of the radical states in the MIMs, we performed cyclic voltammetry (CV) experiments. Upon scanning the potentials up to −600 mV, $\mathbf{1}^{6+}$, $\mathbf{2}^{8+}$, and $\mathbf{M2}^{4+}$ are all reduced to their radical cationic states. In the case of $\mathbf{M2}^{4+}$, both $BIPY^{2+}$ units accept (Figure 2a) simultaneously one electron each at −380 mV. By contrast, $\mathbf{1}^{6+}$ displays (Figure 2b) a stepwise reduction, first undergoing a single-electron reduction at −154 mV to generate $\mathbf{1}^{4+(\bullet+)}$, followed by a double-electron reduction at −294 mV, leading to (Figure 3a) the formation of the tricationic trisradical $\mathbf{1}^{3(\bullet+)}$. It is noteworthy that both of these potential values represent a significant anodic shift when compared with that for $\mathbf{M2}^{4+}$ (−380 mV). The reasons for this shift most likely arise from the nanoconfined geometry and much higher Coulombic repulsion in $\mathbf{1}^{6+}$ destabilizing the molecule, and, compared with radical dimer, $BIPY^{\bullet+}$ radical cations being more stable when they form trisradical trications. In the case of $\mathbf{2}^{8+}$, these two effects are even more pronounced and the outcome is yet more complicated because of the introduction of an additional $BIPY^{2+}$ unit. This octacation first undergoes (Figure 2c) a single-electron reduction to form (Figure 3b)

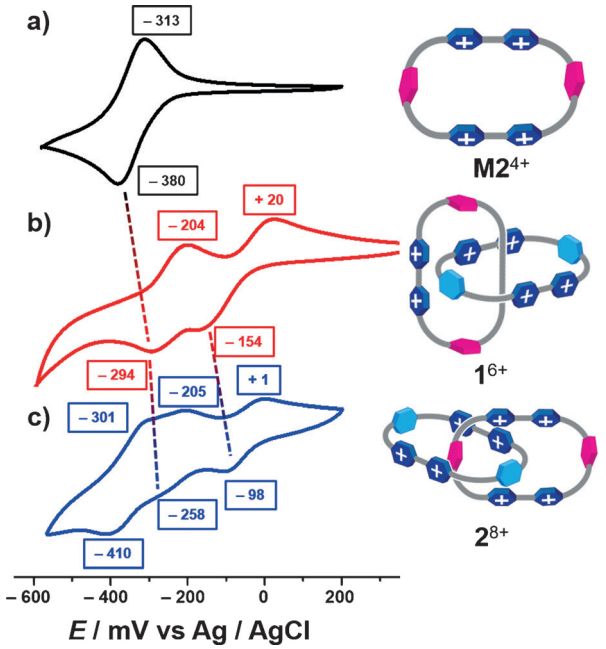

Figure 2. Cyclic voltammograms of a) $\mathbf{M2}^{4+}$, b) $\mathbf{1}^{6+}$, and c) $\mathbf{2}^{8+}$. The dashed lines denote the anodic shifts of the redox peaks as the number of $BIPY^{2+}$ units in the compounds increases. A glassy carbon working electrode, a platinum counter electrode, and a Ag/AgCl reference electrode were used in the characterization of 0.5 mM MeCN solutions of these compounds at 298 K with 0.1 M $TBAPF_6$ serving as the electrolyte. A scan rate of 200 mVs^{-1} was used in all of the analyses.

a mixed-valence state $\mathbf{2}^{6+(\bullet+)}$ at −98 mV, a potential that is shifted even further anodically compared with that for $\mathbf{1}^{6+}$ (−154 mV), presumably because four $BIPY^{2+}$ units result in an even stronger Coulombic repulsion. Next, $\mathbf{2}^{6+(\bullet+)}$ accepts another electron at −258 mV to generate $\mathbf{2}^{4+2(\bullet+)}$, resulting in

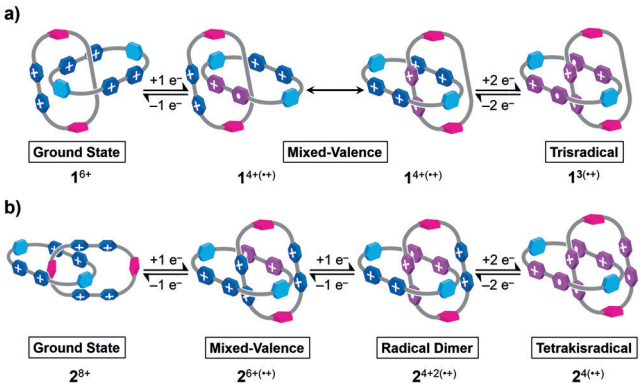

Figure 3. Proposed mechanisms of the stepwise reduction exhibited by the [2]catenanes $\mathbf{1}^{6+}$ (a) and $\mathbf{2}^{8+}$ (b). Firstly, $\mathbf{1}^{6+}$ accepts one electron, leading to the formation of the mixed-valence state $\mathbf{1}^{4+(\bullet+)}$, followed by a concerted double-electron reduction to generate the trisradical complex $\mathbf{1}^{3(\bullet+)}$. By contrast, the reduction of $\mathbf{2}^{8+}$ happens in three successive steps, involving the formation of i) the stable mixed-valence state $\mathbf{2}^{6+(\bullet+)}$, ii) the radical dimer $\mathbf{2}^{4+2(\bullet+)}$, and iii) the tetrakisradical complex $\mathbf{2}^{4(\bullet+)}$. Upon re-oxidation, these reduction processes are fully reversible, resulting in the regeneration of the radical intermediates along paths that lead to the ground states $\mathbf{1}^{6+}$ and $\mathbf{2}^{8+}$. See the Supporting Information, Section 6 for details.

the formation of the intramolecular $(BIPY^{\bullet+})_2$ dimer. Finally, the reduction of the remaining two $BIPY^{2+}$ units occurs simultaneously at −410 mV, leading to the formation of the intramolecular tetracationic tetrakisradical $\mathbf{2}^{4(\bullet+)}$. Differential pulse voltammetry (DPV) experiments (Figure S19) confirmed the number of electrons participating in each step of the reduction of both $\mathbf{1}^{6+}$ and $\mathbf{2}^{8+}$. These observations, along with the results obtained from UV/Vis/NIR spectroscopy, support the formation of intramolecular $BIPY^{\bullet+}$ π-stacks as a consequence of the nanoconfined structures of the [2]catenanes.

The solid-state (super)structure of the trisradical trication $\mathbf{1}^{3(\bullet+)}$ provides some insight into the radical templation that governs its synthesis. The solid-state structure reveals (Figure 4a) that the $CBPQT^{2(\bullet+)}$ ring encircles the $BIPY^{\bullet+}$ unit in

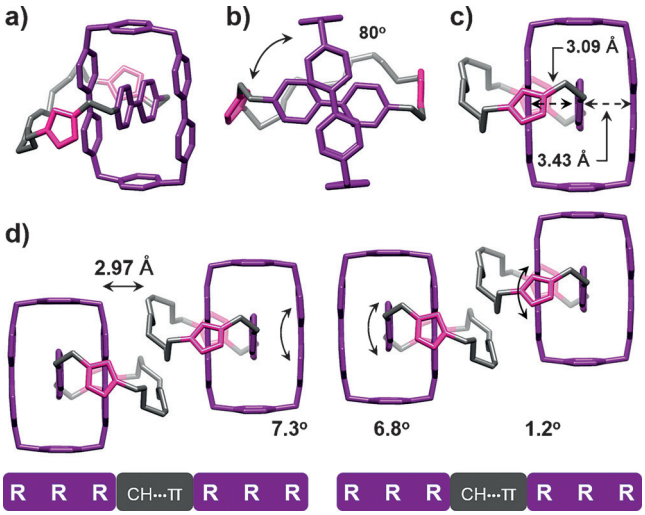

Figure 4. Solid-state (super)structures of the [2]catenane $\mathbf{1}^{3(\bullet+)}$ obtained by single-crystal X-ray crystallography. a–c) Tubular representations of the solid-state structure of $\mathbf{1}^{3(\bullet+)}$ from different perspectives, illustrating the angles and distances associated with adjacent $BIPY^{\bullet+}$ units within a single $\mathbf{1}^{3(\bullet+)}$ molecule. d) A tubular representation of its superstructure, displaying the packing arrangement between adjacent $\mathbf{1}^{3(\bullet+)}$ molecules, where intermolecular [C–H···π] interactions help to control the packing. R denotes the $BIPY^{\bullet+}$ radical cation. The PF_6^- counterions and MeCN solvent molecules have been omitted for the sake of clarity.

the macrocyclic component in order to maximize[9b] radical-pairing interactions. The relative geometry of the $BIPY^{\bullet+}$ unit is such that the encircled unit subtends an angle of 80° with its two neighboring $BIPY^{\bullet+}$ units in the $CBPQT^{2(\bullet+)}$ ring and aligns (Figure 4b) its plane in a parallel fashion with those of the $BIPY^{\bullet+}$ units such that it is (Figure 4c) much closer to one side (3.09 Å) than to the other side (3.43 Å). This geometrical displacement is most likely dictated by the relative positioning of the macrocyclic component. The dihedral angles (Figure 4d) of 1.2, 6.8, and 7.3° associated with the three $BIPY^{\bullet+}$ units are all significantly smaller than those (ca. 20°) characteristic of $BIPY^{2+}$ units, confirming[8b] their radical cationic states. Surprisingly, no intermolecular radical-pairing interactions are present in the packing of the $\mathbf{1}^{3(\bullet+)}$ trisradical tricationic in the crystal. Instead, [C–H···π] interactions exist

between methylene protons in the oligomethylene chain of one catenane molecule and a $BIPY^{(\bullet+)}$ unit in an adjacent trisradical tricationic resulting in alternating radical stacking and [C–H···π] interactions arrayed in a linear fashion. The co-conformation adopted by $\mathbf{1}^{3(\bullet+)}$ is completely in line with its synthesis as a result of the Cu^0-triggered radical templation prior to Cu^I-catalyzed CuAAC reactions.

In summary, we have demonstrated that Cu^0 metal dust can be utilized to reduce viologen units to their radical cationic states. Taking advantage of this discovery, a user-friendly procedure (Table 1), which enables the construction of positively charged catenanes and rotaxanes, templated by radical-pairing interactions in a convenient and efficient manner, has been conceived and implemented. In this procedure, copper metal acts initially as a reducing reagent to generate radical species, during which time Cu^0 is oxidized to Cu^I in situ and goes on to catalyze the CuAAC reaction under radical-templation in high yield. We have shown that this symbiotic effect is crucial to the overall reaction process, and by applying this approach to some carefully chosen target compounds, a series of MIMs composed of dicationic $BIPY^{2+}$ units were prepared. Furthermore, on characterizing these MIMs, both in solution and in the solid-state, we gained a deeper insight into how viologen units can be used in the syntheses of MIMs, where the component parts repel each other as a consequence of the generation of multiple positive charges once they come into contact with the oxygen in air.

Table 1: Comparison of the copper-mediated approach described in this paper with the previously reported ones for preparing viologen-only-based MIMs.

Approach	MIMs	Time [Days]	Yield [%]	Substrate[a] and Catalyst
Copper-Free Click[8a]	Rotaxanes	15–30	≈30	Strained Internal Alkyne[b]
Ring-Clipping[8b]	Catenanes	>14	<30	4,4′-Bipyridine[b]
Olefin-Metathesis[18b]	Catenanes	3	≈30	Terminal Alkene and Additional Catalyst
This Work	Rotaxanes and Catenanes	3	>60	Terminal Alkyne and In Situ Generated Catalyst

[a] Specific structural features required for the syntheses. [b] No catalyst is required for the reaction.

Experimental Section

1·6 PF_6: An excess of Cu dust was added to **4**·2 PF_6 (28 mg, 0.05 mmol) and **CBPQT**·4 PF_6 (55 mg, 0.05 mmol) dissolved in degassed MeCN (20 mL) in an Ar-filled glovebox. After stirring for 20 min, the colorless solution turned dark purple, and a MeCN solution (5 mL) of **6** (12 mg, 0.05 mmol) was added to the reaction mixture, which was stirred for 3 days at room temperature. The solvent was removed by evaporation and the residue purified by column chromatography (SiO_2: 2% w/v MeCN solution of NH_4PF_6 as the eluent). The major component was collected, the solvent removed under vacuum, and the solid re-dissolved in H_2O prior to precipitation with an excess of NH_4PF_6. The precipitate was collected by filtration and washed with H_2O, MeOH, and finally Et_2O to afford **1**·6 PF_6 as a white solid (71 mg, 75%). ^1H NMR (500 MHz, CD_3CN): $\delta = 8.90$ (d, $J = 5.0$ Hz, 4H), 8.87 (d, $J = 5.0$ Hz, 8H), 8.19 (d, $J = 5.0$ Hz, 8H), 7.92 (d, $J = 5.0$ Hz, 4H), 7.75 (s, 2H), 7.05 (s, 8H), 5.50 (s, 8H), 4.92 (t, $J = 7.5$ Hz, 4H), 4.30 (t, $J = 7.5$ Hz, 4H), 3.49 (t, $J = 7.5$ Hz, 4H), 1.44 (p, $J = 7.5$ Hz, 4H), 0.50 (p, $J = 5.0$ Hz, 4H), 0.00 (p, $J = 5.0$ Hz, 4H), −1.61 (m, 4H), −1.72 ppm (p, $J = 5.0$ Hz, 4H). ^{13}C NMR (126 MHz, CD_3CN): $\delta = 148.4$, 147.4, 146.3, 143.7, 136.3, 130.1, 130.1, 127.9, 127.6, 126.5, 124.8, 65.0, 61.7, 50.2, 29.8, 29.4, 29.3, 28.5, 27.0, 26.0 ppm. HRMS (ESI): m/z calcd for $C_{66}H_{74}F_{24}N_{12}P_4$ $[M\text{-}2PF_6]^{2+}$ 807.2363, found 807.2360.

2·8 PF_6: An excess of Cu dust was added to **6**·2 PF_6 (21 mg, 0.025 mmol) dissolved in degassed MeCN (5 mL). Cu Dust in excess was also added to another flask containing **4**·2 PF_6 (14 mg, 0.025 mmol) and **CBPQT**·4 PF_6 (27 mg, 0.025 mmol) which were dissolved in degassed MeCN (10 mL) in an Ar-filled glovebox. After stirring for 20 min, the colorless **6**·2 PF_6 solution turned dark blue and the colorless solution of **4**·2 PF_6 and **CBPQT**·4 PF_6 turned dark purple. Next, the two resulting MeCN solutions were combined. The reaction mixture was stirred for 3 days at room temperature. The solvent was removed by evaporation, and the residue purified by column chromatography (SiO_2: 3% w/v MeCN solution of NH_4PF_6 as the eluent). The major component was collected, the solvent removed under vacuum, and the solid re-dissolved in H_2O prior to precipitation with an excess of NH_4PF_6. The precipitate was collected by filtration and washed with H_2O, MeOH, and finally Et_2O to afford **2**·8 PF_6 as an off-white solid (41 mg, 66%). ^1H NMR (500 MHz, CD_3COCD_3): $\delta =$ 9.50 (d, $J = 5.0$ Hz, 8H), 9.27–9.36 (m, 4H), 8.81 (d, $J = 5.0$ Hz, 8H), 8.62–8.70 (m, 4H), 7.84 (br, 1H), 7.75 (s, 8H), 6.05 (s, 8H), 5.20–5.34 (m, 4H), 4.91–5.02 (m, 8H), 4.35 (t, $J = 7.5$ Hz, 2H), 4.19 (t, $J =$ 7.5 Hz, 2H), 3.52–3.74 (m, 4H), 2.18 (m, 4H), 1.82 (br, 2H), 1.57 (br, 2H), 1.13–1.42 (m, 18H), 0.19 (br, 2H), −0.41 (br, 4H), −1.20 (br, 2H), −1.40 ppm (br, 2H). ^{13}C NMR (126 MHz, CD_3COCD_3): $\delta =$ 150.0, 148.0, 147.8, 147.4, 138.1, 132.3, 129.3, 129.2, 128.8, 128.6, 66.7, 64.2, 64.61, 63.2, 51.0, 28.2, 27.6, 26.9 ppm. HRMS (ESI): m/z calcd for $C_{86}H_{102}F_{36}N_{14}P_6$ $[M\text{-}2PF_6]^{2+}$ 1100.3131, found 1100.3133.

3·6 PF_6: An excess of Cu dust was added to **4**·2 PF_6 (14 mg, 0.025 mmol) and **CBPQT**·4 PF_6 (27 mg, 0.025 mmol) dissolved in degassed MeCN (20 mL) in an Ar-filled glovebox. After stirring for 20 min, the colorless solution turned dark purple, and a MeCN solution (5 mL) of **7** (29 mg, 0.1 mmol) was added to the reaction mixture, which was stirred for 3 days at room temperature. The solvent was removed by evaporation, and the residue was purified by column chromatography (SiO_2: 2% w/v MeCN solution of NH_4PF_6 as the eluent). The major component was collected, the solvent removed under vacuum, and the solid re-dissolved in H_2O, prior to precipitation with an excess of NH_4PF_6. The precipitate was collected by filtration and washed with H_2O, MeOH, and finally Et_2O to afford **3**·6 PF_6 as a white solid (41 mg, 78%). ^1H NMR (500 MHz, CD_3COCD_3): $\delta = 9.55$ (d, $J = 5.0$ Hz, 8H), 9.49 (d, $J = 5.0$ Hz, 2H), 9.38 (d, $J = 5.0$ Hz, 2H), 8.93 (d, $J = 5.0$ Hz, 2H), 8.90 (d, $J = 5.0$ Hz, 2H), 8.85 (d, $J = 5.0$ Hz, 2H), 8.71 (d, $J = 5.0$ Hz, 6H), 8.05 (s, 8H), 8.00 (s, 1H), 7.97 (s, 1H), 7.10–7.20 (m, 6H), 6.21 (dd, $J = 5.0$ Hz, 4H), 6.13 (dd, $J = 5.0$ Hz, 4H), 5.33 (t, $J = 7.5$ Hz, 2H), 5.30 (t, $J = 7.5$ Hz, 2H), 4.90 (m, 2H), 4.67 (t, $J = 7.5$ Hz, 2H), 4.64 (t, $J = 7.5$ Hz, 2H), 3.96 (t, $J = 7.5$ Hz, 2H), 3.93 (t, $J = 7.5$ Hz, 2H), 3.80–3.84 m, 6H), 3.65 (t, $J = 7.5$ Hz, 2H), 3.61 (t, $J = 7.5$ Hz, 2H), 3.32 (septet, $J =$ 7.5 Hz, 4H), 1.21 (d, $J = 5.0$ Hz, 12H), 1.13 ppm (d, $J = 5.0$ Hz, 12H). ^{13}C NMR (126 MHz, CD_3COCD_3): $\delta = 148.0$, 146.4, 145.7, 141.6, 136.9, 130.9, 127.2, 127.0, 126.8, 124.7, 123.9, 123.4, 73.8, 70.2, 69.4, 65.3, 50.0, 27.0, 25.9, 23.7, 23.5 ppm. HRMS (ESI): m/z calcd for $C_{86}H_{100}F_{24}N_{12}O_4P_4$ $[M\text{-}2PF_6]^{2+}$ 972.3279, found 972.3284.

Acknowledgements

This research is part of the Joint Center of Excellence in Integrated Nano-Systems (JCIN) at King Abdulaziz City for Science and Technology (KACST) and Northwestern University (NU). The authors would like to thank both KACST and NU for their continued support of this research.

Keywords: catenanes · click chemistry · radicals · rotaxanes · template-directed synthesis

How to cite: *Angew. Chem. Int. Ed.* **2016**, *55*, 12387–12392
Angew. Chem. **2016**, *128*, 12575–12580

[1] a) J. F. Stoddart, *Chem. Soc. Rev.* **2009**, *38*, 1802–1820; b) S. F. M. van Dongen, S. Cantekin, J. A. A. W. Elemans, A. E. Rowan, R. J. M. Nolte, *Chem. Soc. Rev.* **2014**, *43*, 99–122; c) G. Gil-Ramírez, D. A. Leigh, A. J. Stephens, *Angew. Chem. Int. Ed.* **2015**, *54*, 6110–6150; *Angew. Chem.* **2015**, *127*, 6208–6249.

[2] a) R. Klajn, J. F. Stoddart, B. A. Grzybowski, *Chem. Soc. Rev.* **2010**, *39*, 2203–2237; b) A. C. Fahrenbach, C. J. Bruns, H. Li, A. Trabolsi, A. Coskun, J. F. Stoddart, *Acc. Chem. Res.* **2014**, *47*, 482–493; c) J. Sun, Y. Wu, Z. Liu, D. Cao, Y. Wang, C. Cheng, D. Chen, M. R. Wasielewski, J. F. Stoddart, *J. Phys. Chem. A* **2015**, *119*, 6317–6325.

[3] J. M. Spruell, *Pure Appl. Chem.* **2010**, *82*, 2281–2294.

[4] a) E. R. Kay, D. A. Leigh, F. Zerbetto, *Angew. Chem. Int. Ed.* **2007**, *46*, 72–191; *Angew. Chem.* **2007**, *119*, 72–196; b) C. Cheng, P. R. McGonigal, J. F. Stoddart, R. D. Astumian, *ACS Nano* **2015**, *9*, 8672–8688; c) E. R. Kay, D. A. Leigh, *Angew. Chem. Int. Ed.* **2015**, *54*, 10080–10088; *Angew. Chem.* **2015**, *127*, 10218–10226; d) S. Erbas-Cakmak, D. A. Leigh, C. T. McTernan, A. L. Nussbaumer, *Chem. Rev.* **2015**, *115*, 10081–10206; e) C. Cheng, J. F. Stoddart, *ChemPhysChem* **2016**, *17*, 1780–1793; f) V. Marcos, A. J. Stephens, J. Jaramillo-Garcia, A. L. Nussbaumer, S. L. Woltering, A. Valero, J.-F. Lemonnier, I. J. Vitorica-Yrezabal, D. A. Leigh, *Science* **2016**, *352*, 1555–1559.

[5] Z. Li, J. C. Barnes, A. Bosoy, J. F. Stoddart, J. I. Zink, *Chem. Soc. Rev.* **2012**, *41*, 2590–2605.

[6] P. R. McGonigal, P. Deria, I. Hod, P. Z. Moghadam, A.-J. Avestro, N. E. Horwitz, I. C. Gibbs-Hall, A. K. Blackburn, D. Chen, Y. Y. Botros, M. R. Wasielewski, R. Q. Snurr, J. T. Hupp, O. K. Farha, J. F. Stoddart, *Proc. Natl. Acad. Sci. USA* **2015**, *112*, 11161–11168.

[7] a) S. Anderson, H. L. Anderson, J. K. M. Sanders, *Acc. Chem. Res.* **1993**, *26*, 469–475; b) R. Cacciapaglia, L. Mandolini, *Chem. Soc. Rev.* **1993**, *22*, 221–231; c) R. Hoss, F. Vögtle, *Angew. Chem. Int. Ed. Engl.* **1994**, *33*, 375–384; *Angew. Chem.* **1994**, *106*, 389–398; d) T. J. Hubin, D. H. Busch, *Coord. Chem. Rev.* **2000**, *200*, 5–52; e) Z. R. Laughrey, B. C. Gibb, *Top. Curr. Chem.* **2005**, *249*, 67–125; f) J. D. Crowley, S. M. Goldup, A.-L. Lee, D. A. Leigh, R. T. McBurney, *Chem. Soc. Rev.* **2009**, *38*, 1530–1541; g) A. R. Stefankiewicz, M. R. Sambrook, J. K. M. Sanders, *Chem. Sci.* **2012**, *3*, 2326–2329; h) S. Zhuo, J. Zhang, Y. Shi, Y. Huang, B. Zhang, *Angew. Chem. Int. Ed.* **2015**, *54*, 5693–5696; *Angew. Chem.* **2015**, *127*, 5785–5788.

[8] a) H. Li, A. C. Fahrenbach, S. K. Dey, S. Basu, A. Trabolsi, Z. Zhu, Y. Y. Botros, J. F. Stoddart, *Angew. Chem. Int. Ed.* **2010**, *49*, 8260–8265; *Angew. Chem.* **2010**, *122*, 8436–8441; b) J. C. Barnes, A. C. Fahrenbach, D. Cao, S. M. Dyar, M. Frasconi, M. A. Giesener, D. Benítez, E. Tkatchouk, O. Chernyashevskyy, W. H. Shin, H. Li, S. Sampath, C. L. Stern, A. A. Sarjeant, K. J. Hartlieb, Z. Liu, R. Carmieli, Y. Y. Botros, J. W. Choi, A. M. Z. Slawin, J. B. Ketterson, M. R. Wasielewski, W. A. Goddard III, J. F. Stoddart, *Science* **2013**, *339*, 429–433.

[9] a) A. Trabolsi, N. Khashab, A. C. Fahrenbach, D. C. Friedman, M. T. Colvin, K. K. Cotí, D. Benítez, E. Tkatchouk, J. C. Olsen, M. E. Belowich, R. Carmielli, H. A. Khatib, W. A. Goddard III, M. R. Wasielewski, J. F. Stoddart, *Nat. Chem.* **2010**, *2*, 42–49; b) A. C. Fahrenbach, J. C. Barnes, D. A. Lanfranchi, H. Li, A. Coskun, J. J. Gassensmith, Z. Liu, D. Benítez, A. Trabolsi, W. A. Goddard III, Elhabiri, M. , J. F. Stoddart, *J. Am. Chem. Soc.* **2012**, *134*, 3061–3072.

[10] a) J. M. Spruell, A. Coskun, D. C. Friedman, R. S. Forgan, A. A. Sarjeant, A. Trabolsi, A. C. Fahrenbach, G. Barin, W. F. Paxton, S. K. Dey, M. A. Olson, D. Benítez, E. Tkatchouk, M. T. Colvin, R. Carmielli, S. T. Caldwell, G. M. Rosair, S. G. Hewage, F. Duclairoir, J. L. Seymour, A. M. Z. Slawin, W. A. Goddard III, M. R. Wasielewski, G. Cooke, J. F. Stoddart, *Nat. Chem.* **2010**, *2*, 870–879; b) Z. Zhu, A. C. Fahrenbach, H. Li, J. C. Barnes, Z. Liu, S. M. Dyar, H. Zhang, J. Lei, R. Carmieli, A. A. Sarjeant, C. L. Stern, M. R. Wasielewski, J. F. Stoddart, *J. Am. Chem. Soc.* **2012**, *134*, 11709–11720.

[11] C. Cheng, P. R. McGonigal, S. T. Schneebeli, H. Li, N. A. Vermeulen, C. Ke, J. F. Stoddart, *Nat. Nanotechnol.* **2015**, *10*, 547–553.

[12] a) V. V. Rostovtsev, L. G. Green, V. V. Fokin, K. B. Sharpless, *Angew. Chem. Int. Ed.* **2002**, *41*, 2596–2599; *Angew. Chem.* **2002**, *114*, 2708–2711; b) C. W. Tornøe, C. Christensen, M. Meldal, *J. Org. Chem.* **2002**, *67*, 3057–3064.

[13] K. D. Hänni, D. A. Leigh, *Chem. Soc. Rev.* **2010**, *39*, 1240–1251.

[14] P. R. Ashton, P. T. Glink, J. F. Stoddart, P. A. Tasker, A. J. P. White, D. J. Williams, *Chem. Eur. J.* **1996**, *2*, 729–736.

[15] R. Huisgen, *Pure Appl. Chem.* **1989**, *61*, 613–628.

[16] a) P. Appukkuttan, W. Dehaen, V. V. Fokin, E. Van der Eycken, *Org. Lett.* **2004**, *6*, 4223–4225; b) F. Himo, T. Lovell, R. Hilgraf, V. V. Rostovtsev, L. Noodleman, K. B. Sharpless, V. V. Fokin, *J. Am. Chem. Soc.* **2005**, *127*, 210–216; c) C. N. Urbani, C. A. Bell, M. R. Whittaker, M. J. Monteiro, *Macromolecules* **2008**, *41*, 1057–1060.

[17] a) S. J. Loeb, *Chem. Soc. Rev.* **2007**, *36*, 226–235; b) X. Ma, H. Tian, *Chem. Soc. Rev.* **2010**, *39*, 70–80; c) M. Xue, Y. Yang, X. Chi, X. Yan, F. Huang, *Chem. Rev.* **2015**, *115*, 7398–7501.

[18] a) N. H. Evans, P. D. Beer, *Chem. Soc. Rev.* **2014**, *43*, 4658–4683; b) I. C. Gibbs-Hall, N. A. Vermeulen, E. J. Dale, J. J. Henkelis, A. K. Blackburn, J. C. Barnes, J. F. Stoddart, *J. Am. Chem. Soc.* **2015**, *137*, 15640–15643.

[19] a) S. Hünig, *Pure Appl. Chem.* **1967**, *15*, 109–122; b) E. M. Kosower, J. Hajdu, *J. Am. Chem. Soc.* **1971**, *93*, 2534–2535; c) T. M. Bockman, J. K. Kochi, *J. Org. Chem.* **1990**, *55*, 4127–4135.

Received: June 4, 2016
Revised: July 16, 2016
Published online: September 8, 2016

